







RETINOL DISPERSION IN THE FORM OF HYDROGEL FOR DERMAL DELIVERY

Ioana Lavinia LIXANDRU MATEI^{a,b} ,
Bogdan Alexandru SAVA^{b,c,*} , Andreea Iuliana IONESCU^a,
Codruta SAROSI^d , Gabriel VASILIEVICI^e ,
Marian BĂJAN^f , Daniela Luminița MOVILEANU^f ,
Daniela Roxana POPOVICI^f , Abeer BAOUNF^g

ABSTRACT. This study reports the development of a dermato-cosmetic hydrogel combining retinol (2% wt) and bioactive glass (1.25% wt) in a Carbopol-based matrix enriched with hyaluronic acid. The formulation was synthesized using high-shear dispersion and evaluated through TGA, DSC, FTIR, and XRD. Thermal analysis indicated strong water-polymer interactions, while FTIR and XRD confirmed amorphous structure favorable for controlled release. The hydrogel showed high conductivity (25000 $\mu\text{S}/\text{cm}$) and alkaline pH (12.4), attributed to its 85% water and triethanolamine content. Turbiscan and microscopy confirmed physical stability. Microbiological tests confirmed sterility. In vivo VISIA analysis on five volunteers over 45 days revealed visible improvements in wrinkles, pores, red areas, UV spots, and porphyrins, with notable changes as early as day 14. These results support the hydrogel's potential for effective and well-tolerated dermal delivery of retinol.

Keywords: retinol, hydrogel, dermal delivery, stability, bioglass

^a Botanical SRL, 7 Trandafirilor St., Tatarani, Prahova County, 107059 Romania.

^b University Politehnica Bucharest Splaiul Independenței, 060042 Bucharest, Romania.

^c National Institute of Laser, Plasma and Radiation Physics - INFLPR 409 Atomistilor St., Magurele, Jud. Ilfov, Romania.

^d Babes-Bolyai University, 1 Mihail Kogălniceanu St., 400084 Cluj-Napoca, Romania.

^e National Institute for Research Development for Chemistry and Petrochemistry-ICECHIM-Bucuresti, 202 Spl. Independentei, 060021 Bucharest, Romania.

^f Petroleum-Gas University of Ploiesti, Faculty of Petroleum Refining and Petrochemistry, 39 Bucharest Boulevard, 100515 Ploiesti, Romania.

^g Chemistry Department, Faculty of Science, University of Damascus, Damascus, Syria.

* Corresponding author: bogdan.sava2901@upb.ro



INTRODUCTION

Retinol is an essential component in dermatological therapies due to its ability to stimulate skin renewal, increase collagen production, and improve the appearance of skin affected by photoaging and acne. However, its clinical use is often limited by side effects, including redness, dryness, and irritation, particularly in those with sensitive skin or weakened epidermal barriers.

To address these negative effects and improve the tolerability of retinoid treatments, new formulation techniques have been introduced. One innovative approach is the use of bioactive glass, a biocompatible substance recognized for its regenerative and anti-inflammatory properties. This material not only aids in skin regeneration but also allows for the controlled release of active ingredients, thereby minimizing irritation and enabling higher doses of retinoids to be used without damaging skin integrity [1- 6].

In a recent case series, Tran Thuy Len et al. assessed the effectiveness of herbal oil-based extracts from *Bambusa vulgaris* (bamboo) leaves as a topical remedy for atopic dermatitis. The findings demonstrated that bamboo leaf extract, when paired with appropriate carriers, significantly alleviated symptoms of atopic dermatitis, such as redness and itching, across various patient demographics. This underscores the potential of incorporating bioactive compounds into dermocosmetic products to enhance therapeutic effectiveness [7].

Another promising approach involves the development of silicone particles specifically designed for encapsulating and controlling the release of retinol. Research conducted by Nasrin Ghouchi Eskandar and colleagues demonstrated that silicone particles created through sol-gel polymerization can effectively encapsulate retinol, safeguarding it from degradation while facilitating its gradual release. This delivery system enhances retinol's stability and minimizes the potential for irritation, thereby offering a more user-friendly option for topical applications [8].

A study conducted by Cook et al. assessed a novel topical formulation that merges retinol with a natural peptide derived from peas and an antioxidant blend. In vitro tests demonstrated an increase in key skin biomarkers, including aquaporin-3, collagen, and elastin, while also reducing the expression of pigmentation-related genes. Clinically, this formulation significantly improved skin hydration, elasticity, and overall appearance without causing irritation [9].

The research conducted by Shields et al. investigated the encapsulation and controlled release of retinol using silicone particles for topical delivery. The authors introduced a novel category of silicone particles created through the sol-gel polymerization of silane monomers, enabling rapid and scalable production with a uniform size distribution (coefficient of variation <20%).

These particles demonstrated a high encapsulation efficiency of over 85% for retinol and significantly improved its stability, with a half-life nine times longer than that of unencapsulated retinol. The study also noted that these silicone particles could encapsulate other active ingredients, highlighting their versatility as a platform for topical drug delivery. This research underscores the potential of silicone particle-based systems in enhancing the stability, controlled release, and tolerability of retinol within dermocosmetic formulations [10].

Kim et al. developed low molecular weight, water-soluble chitosan nanoparticles to encapsulate retinol, achieving over a 1600-fold increase in solubility compared to free retinol. The nanoparticles were spherical in shape, with sizes ranging from 50 to 200 nm, and encapsulation was accomplished through ion complex formation between chitosan and retinol. This method enhanced the stability of retinol, as demonstrated by the absence of its characteristic peaks in Fourier-transform infrared (FT-IR) and nuclear magnetic resonance (NMR) spectroscopy. Moreover, X-ray diffraction (XRD) analysis revealed that the crystalline structure of retinol was modified during encapsulation, indicating a transition to an amorphous state that may improve both stability and bioavailability. These findings underscore the potential of chitosan nanoparticles as an effective delivery system to enhance the stability and solubility of retinol for dermocosmetic applications [11].

Laredj-Bourezga et al. investigated surfactant-free Pickering emulsions stabilized by biodegradable block copolymer micelles—specifically, poly(lactide)-block-poly(ethylene glycol) (PLA-b-PEG) and poly(caprolactone)-block-poly(ethylene glycol) (PCL-b-PEG)—for the targeted delivery of hydrophobic drugs such as all-trans retinol. The emulsions were formulated using two distinct approaches: one method involved encapsulating the drug within oil droplets, while the other incorporated the drug both within oil droplets and within non-adsorbed block copolymer nanoparticles. In vitro skin absorption tests utilizing pig skin biopsies and the Franz cell method, supplemented by confocal fluorescence microscopy, demonstrated that these Pickering emulsions resulted in significantly greater accumulation of retinol in the stratum corneum compared to traditional surfactant-based emulsions and oil solutions. Moreover, loading the drug within both oil droplets and block copolymer nanoparticles enhanced skin absorption, attributed to the additional effects of the free block copolymer nanoparticles containing the drug. This innovative approach facilitates customizable drug delivery to the skin, offering a promising strategy for improving the efficacy and stability of retinol in dermocosmetic formulations [12,13].

Mahmood and Shipman offer a historical perspective on acne vulgaris, emphasizing its persistent presence and the evolving understanding of the condition throughout medical history. The authors trace the acknowledgment

of acne back to ancient civilizations, citing its mention in the Ebers Papyrus from ancient Egypt and its connection to puberty in ancient Greek writings. The article delves into various theories surrounding the causes of acne, including hormonal factors, dietary influences, and hygiene practices, reflecting the changing viewpoints over time. A substantial portion of the discussion is devoted to the discovery and development of retinoids, particularly isotretinoin, highlighting their transformative impact on acne treatment and the pertinent considerations for women's health, especially in relation to pregnancy. The authors conclude by acknowledging the advancements made in acne treatment while also addressing ongoing challenges and the need for continued research in this area [14].

Im et al. conducted a randomized, double-blind, placebo-controlled split-face trial to evaluate the efficacy of a topical herbal cream based on Sasang constitutional medicine for reducing wrinkles in individuals with the So-eum (SE) type. This herbal formulation, which includes a blend of *Zingiber officinale*, *Atractylodes chinensis*, *Curcuma longa*, and *Cinnamomum cassia* (referred to as ZACC extract), was applied to the faces of 21 SE-type participants over a period of 12 weeks. The results revealed significant improvements in skin roughness (R1) and smoothness depth (R4) in the treated areas compared to the placebo, with no reported adverse dermatological reactions. These findings suggest that the ZACC herbal cream may effectively prevent or slow skin aging, including the development of wrinkles, in individuals of the SE type [15].

Building on these findings, the current study explores the effectiveness of a novel dermocosmetic formulation that combines retinol, infused in bioactive glass, to enhance skin appearance. This formulation aims to leverage the synergistic effects of retinol's skin-renewing properties alongside the regenerative capabilities of bioactive glass, providing a promising solution for those seeking effective and tolerable skin rejuvenation treatments. The novelty elements are given by the use of two competing mechanisms for the delayed release of retinol on the surface of the epidermis, namely the reduction of diffusion in the fluid phase by increasing the viscosity of the respective product and the adsorption of retinol in the pores of a powdered adsorbent. Thus, the increase in viscosity was achieved by transforming the retinol solution into a hydrogel based on hyaluronic acid and a copolymer of the Carbopol Aqua SF-1 OS type. The adsorbent used for the controlled release is powdered bioglass, a non-crystalline amorphous solid with various uses in the cosmetic and medical fields.

RESULTS AND DISCUSSION

Thermal Properties

The hydrogel demonstrated a pronounced mass loss during the initial portion of the TGA curve (Figure 1), specifically within the temperature range of 40 °C to 130 °C, with a peak mass loss observed on the differential thermogravimetric (DTG) curve around 125 °C. This significant mass loss is primarily attributed to the evaporation of water. In the subsequent heating phase, spanning from 130 °C to 230 °C, the rate of mass loss diminished, with the maximum loss recorded on the DTG curve at approximately 225 °C. This phenomenon is likely due to the evaporation of various volatile organic compounds, including triethanolamine (TEA). Beyond 230 °C, further mass losses were noted, albeit at a reduced rate, with no additional maxima detected in this temperature range. These losses can be ascribed to both the evaporation of organic compounds carried by the inert gas and the thermal degradation of non-volatile organic constituents such as hyaluronic acid, retinol, and the Carbopol Aqua SF-1 OS polymer, as was suggested by Altaieb [16].

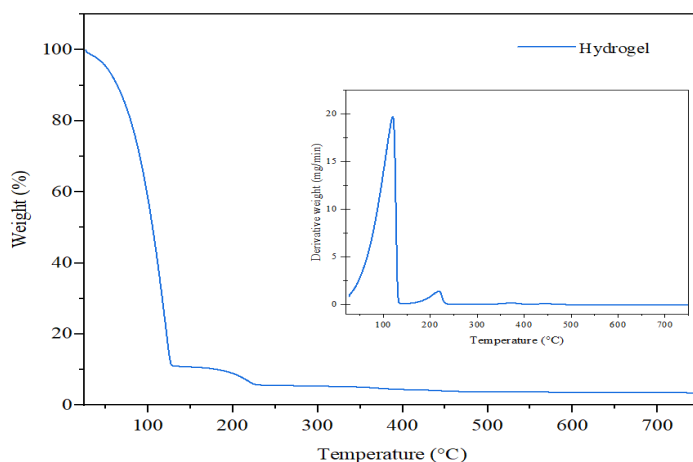


Figure 1. Thermogravimetric analysis of the hydrogel

The impact of the physicochemical characteristics of cosmetic hydrogel on thermal transitions is elucidated through the Differential Scanning Calorimetry (DSC) thermogram, as depicted in Figure 2. Notably, the initial segment of the curve reveals an endothermic peak, characterized by a maximum that occurs at temperatures of approximately 120 °C, attributed to the evaporation of water [17]. The endothermic inflexion point observed at 97 °C is probably indicating a transition within the amorphous matrix. The temperature at which this endothermic

peak is observed is influenced by the nature of the interactions between water molecules and other constituents present in the formulation. The hydrophilic polymer employed in the hydrogel formulation facilitates the retention of water molecules through hydrogen bonding and electrostatic interactions [18,19].

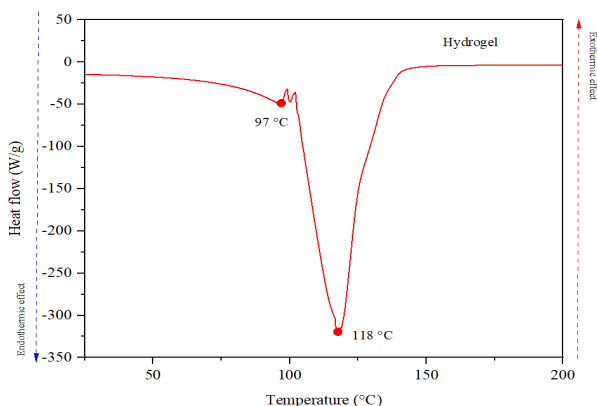


Figure 2. DSC thermogram of the hydrogel

FTIR Analysis

The results of the FTIR analysis, illustrated in Figure 3, reveal that the stretching vibrations observed at 3321 cm^{-1} are associated with the O-H bonds found in both water and triethanolamine (TEA). The presence of amine groups is indicated by the absorption peak at 1639 cm^{-1} , specific to the bending vibrations of the N-H bonds in these functional groups. The existence of carbon in paraffinic structures is indicated by a weak peak at 2085 cm^{-1} , specific to the stretching vibrations of the C-H bonds in methyl or methylene groups.

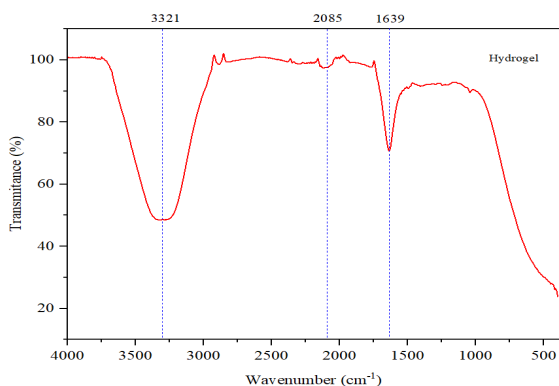


Figure 3. The FTIR spectra of the hydrogel

In the hydrogel, the shift of this band toward lower wavenumber values can be attributed to the incorporation of retinol [20].

XRD Analysis

The hydrogel (Figure 4) exhibits a predominantly amorphous structure, as indicated by X-ray diffraction (XRD) analysis. The XRD pattern reveals a broad and relatively weak peak in the range of 30° to 35° . This characteristic shape of the single broadened peak is consistent with the presence of bioglass, further supporting its classification as an amorphous material [1]. The lack of crystalline structures within the hydrogel is a critical attribute desired in the formulation of this material, as it facilitates the regulated release of nutrients. This characteristic enhances the hydrogel's efficacy in various applications, particularly in controlled delivery systems, by allowing for a more consistent and sustained liberation of active compounds.

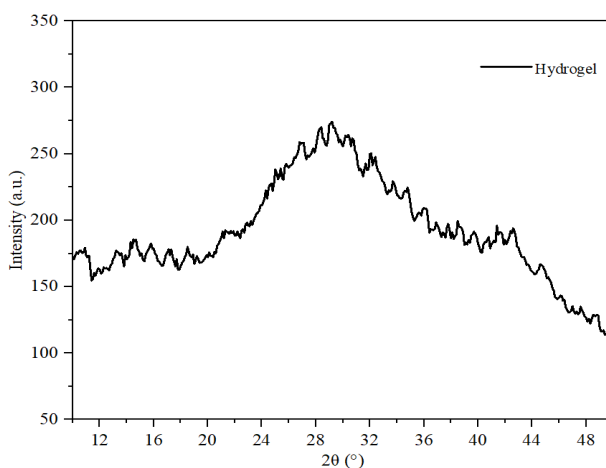


Figure 4. XRD spectra of the hydrogel

Electrical Conductivity and pH

The conductivity and pH values of the sample are the main physical characteristics of the hydrogel. It is evident that the hydrogel demonstrates a relatively high conductivity attributed to its high content of acrylic copolymer in ionized form (25000 $\mu\text{S}/\text{cm}$). That value sufficient mimicking electrical conductivity of some human tissues [21-23]. The hydrogel exhibits a higher pH value, which can be attributed to triethanolamine and acrylates content.

Stability Tests

We examined the variation in backscattering relative to the height of the container holding the analyzed sample, as well as the changes observed over a period of 6 hours with periodic measurements taken each hour. Across all samples, sedimentation was noted in the lower part of the container, with low backscattering values indicating the presence of sediment. At container heights exceeding 10%, backscattering exhibited a marked increase and tended to stabilize throughout the container's height. The maximum backscattering value for the hydrogel was approximately 23%, indicating a low concentration of particles within the sample (refer to Figure 5). For container heights greater than 10 mm, the backscattering curve showed variations within a narrow range of less than 2%, suggesting a relatively high stability of the hydrogel-based dispersion. Additionally, a modest decrease in backscattering over the 6-hour period was observed, amounting to less than 2%. This decline in signal indicates a degree of instability in the hydrogel-based dispersed system.

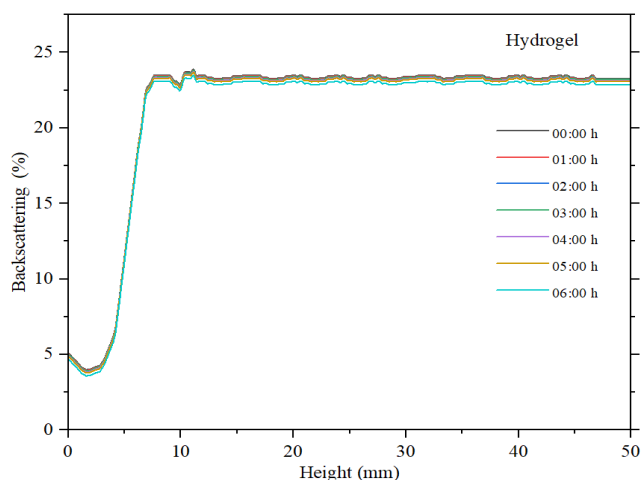


Figure 5. Backscattering curve for hydrogel

Hydrogel Droplet Size

Microscopic analyses performed at 160× magnification revealed visible hydrogel droplets predominantly in the size range of 300 to 900 μm . While finer details below this range cannot be resolved with optical microscopy at this magnification, the observed reduction in the apparent abundance of smaller droplets over time suggests coalescence or phase destabilization

phenomena at the microscale. Therefore, the “small droplets” abundance was assessed in a relative manner, based on droplet size appearance and distribution patterns observable under the given optical conditions. This interpretation has been updated accordingly in the discussion section to reflect the physical resolution limits of the employed optical system. (See Figure 6). The formulation was monitored for stability over a period of six hours after preparation, with an intermediate measurement taken at the three-hour mark. A slight trend toward droplet aggregation was observed over time, reflected by a gradual decrease in the proportion of small-sized droplets. The maximum estimation error was found to be 2.3%, based on sample analysis.

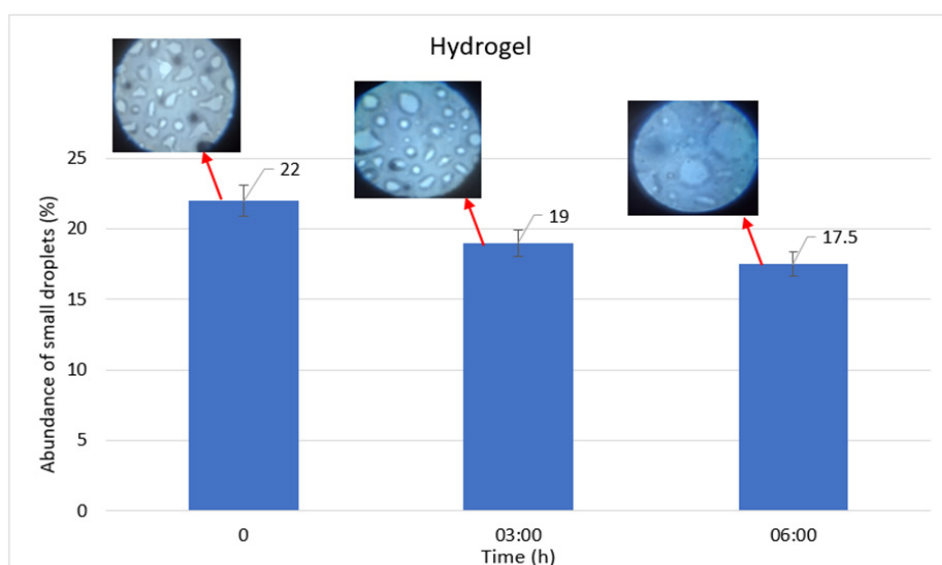


Figure 6. Evolution of the abundance of small droplets in the hydrogel formulation over a 6-hour period, measured at 0, 3, and 6 hours' post-preparation and their microscopically aspect at magnification of 160x.

Dermal Delivery Tests

The hydrogel prepared in the laboratory was applied by five volunteers (one male and four females) over a period of 45 days. The effectiveness of the hydrogel was evaluated using the advanced VISIA imaging system. Thus, a computerized dermal analysis of the skin was performed with the VISIA system.

The parameters obtained from this assessment included wrinkles, texture, pores, and the effects of sun exposure (UV spots, brown spots, and red areas). All tests were conducted in-house (at the Plush Bio laboratory).

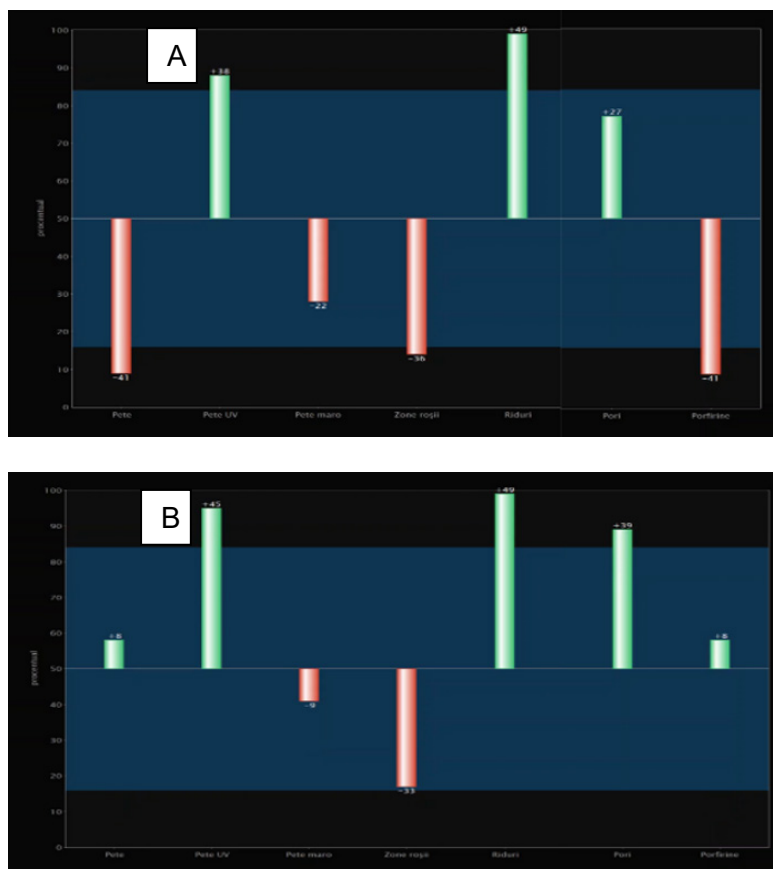


Figure 7. Comparative chart for relative scores: (A) start date – (B) end date

Figure 7 shows the skin evolution of one of the volunteers over a two-week period. The 3D scan captured by the VISIA system indicates a significant improvement in the red areas of the skin.

A comparative progression can thus be observed in terms of UV spots, brown spots, red areas, and porphyrins between the initial and final evaluations (Figure 8).

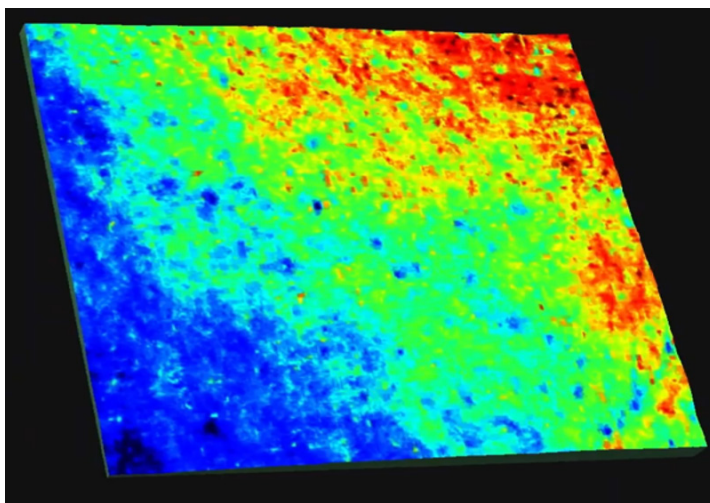


Figure 8. 3D VISIA scan illustrating skin parameter changes after two weeks of hydrogel application.

Discussion

The study investigates the characteristics of dermato-cosmetic formulation, specifically hydrogels, which synergistically incorporate bioglass and retinol. The objective is to mitigate the irritant potential of retinoids while prolonging their therapeutic efficacy for applications within the health and cosmetics industries. A multifaceted approach employing various characterization methods has been utilized to analyze these formulations comprehensively. Analytical techniques, including thermogravimetric analysis (TGA), differential scanning calorimetry (DSC), and X-ray diffraction (XRD), were employed alongside stability. The results indicate that the electrical conductivity of the formulation is influenced by the polarity of the polymer. Thus, the hydrogel exhibited markedly a higher conductivity. The pH values of the formulation were mainly determined by the content of triethanolamine (TEA) in the continuous phase. TGA and DSC analyses suggested a significant change in the temperature at which maximum water loss occurred, indicating strong interactions between water molecules and the polymer present in the hydrogel. Fourier-transform infrared (FTIR) spectroscopy confirmed the presence of Si-O-Ca and Si-O-Si bonds, at 1100 cm^{-1} , consistent with the incorporation of bioglass. XRD analysis was conducted to evaluate the crystallinity of the prepared materials, allowing for a quantitative assessment of any crystalline phases present, including those associated with the bioglass or organic

compounds with high melting points. The absence of diffraction peaks corresponding to oxide structures suggests a completely amorphous structure of the utilized bioglass. Stability analysis of the hydrogel, assessed by backscattering measurements, revealed a relatively low value of backscattering, indicating a low concentration of dispersed particles. The hydrogel demonstrated high stability over a period of six hours, evidenced by minimal variations in backscattering. The skin delivery test performed with the VISIA system to evaluate wrinkles, texture, pores and the effects of sun exposure, such as UV spots, brown spots and red areas, demonstrated a clear progress especially in terms of UV spots, brown spots, red areas and porphyrins compared to the initial evaluation.

CONCLUSIONS

The conditioning of retinol in the presence of bioglass in the form of a hydrogel represents a promising conditioning method for dermatological and cosmetic applications. Thermal and XRD analyses did not indicate the formation of crystalline structures that could hinder the controlled release of retinol. In addition, stability studies performed using the Turbiscan method and optical microscopy demonstrated that the hydrogel exhibits high stability over time. The proposed hydrogel composition showed high efficiency in treating wrinkles, UV spots, brown spots and red areas, where an obvious progress was noted.

EXPERIMENTAL SECTION

Materials and Reagents

Retinol (Merck, $\geq 95.0\%$), Bioglass® powder Schott (NovaMin USA), hyaluronic acid - HA (Oligo-HA4, Sigma-Aldrich), Carbopol Aqua SF-1 OS Polymer (Lubrizol) triethanolamine - TEA (Merck, reagent grade, 97%), and ultra-pure water, WIFI quality water (Pixico, Romania) were used for the synthesis of hydrogel.

Synthesis of Hydrogel

A hydrogel was prepared through mechanical stirring using an IKA 18 ULTRA-TURRAX digital disperser (IKA-Werke GmbH & Co. KG, Staufen,

Germany) at a speed of 9000 rpm and a temperature of 40 °C for a duration of 30 minutes. The composition and concentration of the components in the resulting hydrogel are outlined in Table 1.

Table 1. Recipes of the hydrogel

Component	Hydrogel (%wt.)
Distilled water	85.00
TEA	5.00
Retinol	2.00
Bioglass	1.25
Hyaluronic acid	0.50
Carbopol Aqua SF-1 OS	6.25

Characterization Methods

The following analyses were performed for the hydrogel obtained in the study: thermogravimetric analysis (TGA), differential scanning calorimetry (DSC), Fourier transform infrared spectroscopy (FTIR), X-ray diffraction (XRD), electrical conductivity, pH, stability analyses, and microbiological analyses.

Thermogravimetric analysis for DE, RE and hydrogel were performed with Thermal Analysis System TGA 2 apparatus from METTLER TOLEDO (Greifensee, Switzerland), in the 25–700 °C temperature range, in a nitrogen atmosphere, with a heating rate of 10 °C/min.

Differential scanning calorimetry was performed to investigate temperature in-duced transitions. The analysis was conducted using a Thermal Analysis System DSC 3+ from Mettler Toledo (Greifensee, Switzerland). The samples were heated from room temperature to 400 °C at a rate of 1 °C per minute in a nitrogen atmosphere.

For the qualitative analysis of the materials, Fourier Transform Infrared was used to identify the functional groups present in the structures. The analysis was conducted using a Shimadzu IRAffinity-1S spectrophotometer (Kyoto, Japan), which was equipped with the GladiATR-10 accessory. The measurements were taken within the wavelength range of 380 to 4000 cm⁻¹, with a spectral resolution of 4 cm⁻¹.

Determination of the conductivity and pH of the hydrogel was performed with the inoLab Multi 9630 IDS (Germany) multimeter. The electrode used for pH is SeTix 980 with glass rod and temperature sensor. The conductivity cell was WTW IDS TetraCon 925.

The degree of crystallinity of the prepared materials was determined by X-ray diffraction performed with a Bruker X-ray diffractometer (Bruker-AXS, Karlsruhe, Germany) equipped with a Cu-K α source at 40 kV and 5 mA, 2 θ range 10°– 50° at a rate of 1 °/ minute.

The stability of the hydrogel was evaluated using the Turbiscan Lab Expert Formulation (Toulouse, France). This provided insights into the tendencies of sedimentation, coalescence, or aggregation of the components in the hydrogel recipe. The colloidal stability of the studied systems was achieved by measuring the backscattering diffusion. Thus, by measuring the amount of light scattered back by the particles in emulsions or hydrogel, the tendency of their stability to change over time is evaluated.

Microscopic visualization of particle abundance was evaluated using a CELESTRON Microscope (Celestron, Torrance, CA, USA), model 4434, along with a Thoma Marienfeld counting chamber. Particles were visualized with green G53 and blue filters AE5202 within a magnification range of 40X to 160X, following an appropriated method [24,25]. Dermal analysis was performed computerized with the VISIA system.

Statistical Analysis

Both the pH and electrical conductance stability were evaluated through three consecutive measurements. The results were subsequently used to calculate experimental errors using the standard deviation statistical function, which provides insight into the dispersion of the data around the mean values. To assess whether the standard deviation is high or low, indicating that the values are either widely varied or closely clustered around the mean, the coefficient of variation was employed [26].

REFERENCES

1. I. L. Lixandru Matei; B. A. Sava; C. Sarosi; C. Duşescu-Vasile; D. R. Popovici; A. I. Ionescu; D. Bomboş; M. Băjan; R. Doukeh; *Nanomaterials*; **2024**, *14*, 1323.
2. M.M. Don; C. Y.San; J .Jeevanandam; Chapter 8 - Antimicrobial properties of nanobiomaterials and the mechanism, in *Nanobiomaterials in Antimicrobial Therapy Applications of Nanobiomaterials*; 1st Edition, Elsevier Inc. All, **2016**, *6*, 261-312.

3. J.R. Jones; D. S. Brauer; L. Hupa; D. C. Greenspan; *Inter.J. of Appl. G. Sci.*, **2016**, 7, 405-544.
4. L. L. Hench; *New Journal of Glass and Ceramics*; **2013**, 3, 67-73.
5. EP1272144A4/**2006**, New cosmetic body cleaning agent and food supplements containing bioactive glass and methods for the preparation and use there of; *European Patent Office*, <https://patents.google.com/patent/EP1272144A4/en>, accessed at 11.06.2025.
6. M. Matinfar; A. Elias ; J. A. Nychka; *Materials & Design*; **2025**, 253, 113919.
7. T.T. Len; H. N. Nhung; T. C.Thanh; *Phytomedicine Plus*, **2023**, 3, 100480.
8. N. G. Eskandar; S. Simovic; C. A. Prestidge; *Int. J. of Pharma*, **2009**, 376, 186-194.
9. B. Cook; M. Riggs; K.C. Holley; *Dermatol Ther (Heidelb)*, **2025**, 15, 189–200.
10. C. Wyatt Shields; J. P. White; E. G. Osta; J. Patel; S. Rajkumar; N. Kirby; J.-P. Therrien; S. Zauscher; *J. of Contr. Rel.*, **2018**, 278, 37-48.
11. D. G. Kim; Y.I. Jeong; C. Choi; S.H. Roh; S.K. Kang; M.K. Jang; J.W. Nah; *Inter. J. of Pharma*, **2006**, 319, 130-138.
12. F. Laredj-Bourezg; M.A.Bolzinger; J. Pelletier; J.P. Valour; M.R. Rovère; B. Smatti; Y. Chevalier; *Inter. J. of Pharma.*, **2015**, 496, 1034-1046.
13. F. Nicolescu; F. Lupu; O Pantea; C.G. Gheorghe; A. Bondarev; C. Calin; *Rev. Chim.*, **2015**, 66, 1181-1183.
14. N.F. Mahmood; A.R. Shipman; **2017**, 3, 71-76.
15. A.R. Im; K.Y. Ji; J. Nam; J. Yoon; S. Cha; Y. K. Seo; S. Chae; J. Y. Kim; *Integrative Medicine Research*, **2022**, 11, 100752.
16. H.A. Altaieb; *J.of Sau. Chem. Soc.*, **2024**, 28, 101852.
17. P. Ahmadi; A. Ahmadi; M. Tabibiazar; S. Hamidi; S. Ramezani; *Carbohydr Polym*, **2025**, 353, 12324.
18. E.Verni; F. Sabatini; C. Lee; G. Fiocco; M. L.Weththimuni; B.Vigani; H. Lange; M. Malagodi; F. Volpi; *Carbohydr. Polym. Tech.s and Appl.*, **2025**, 100875.
19. Y. Enomoto-Rogers; Y. Ohmomo; T. Iwata; *Carbohydr. Polym*, **2013**, 92, 1827–1834.
20. W.Chieng; N.A. Ibrahim; W. M. Z. W. Yunus; M. Z. Hussein; *Polym*, **2014**, 6, 93-104
21. H. Xu; J.M. Holzwarth; Y. Yan; P. Xu; H. Zheng; Y. Yin; S. Li; P.X. Ma; *Biomat*, **2014**, 35, 225–235
22. C. Ramon; P. Gargiulo; E.A. Fridgeirsson; J. Haeisen; *Front. Neuroeng*; **2014**, 7, 32
23. E. V. Parfenyuk; E.S. Dolinina; *Mat. Chem. and Phys.*, **2025**, 342, 130981
24. V. Gheorghe; C.G. Gheorghe; A. Bondarev; R. Somoghi; *Toxics*, **2023**, 11, 285
25. V. Gheorghe; C.G. Gheorghe; D.R. Popovici; S.Mihai; C. Calin; E.E. Sarbu; R. Doukeh; V. Matei; N. Grigoriu; C.N.Toader; C. Epure; *Toxics*, **2023**, 11, 672.
26. D.R. Popovici; C.G. Gheorghe; C.M. Duşescu-Vasile; *Bioengineering*, **2024**, 11, 1306.

